Surface reconstruction and magnesium incorporation on semipolar GaN(1$\bar{1}$01) surfaces

Toru Akiyama,* Daisuke Ammi, Kohji Nakamura, and Tomonori Ito
Department of Physics Engineering, Mie University, 1577 Kurima-Machiya, Tsu 514-8507, Japan
(Received 13 February 2010; revised manuscript received 28 May 2010; published 17 June 2010)

Reconstructions and Mg incorporation on GaN surfaces in semipolar (1$\bar{1}$01) orientation are systematically investigated by performing first-principles pseudopotential calculations. The calculated surface phase diagrams demonstrate that there are several reconstructions depending on the growth conditions. When the pressure of H_2 is low, the surface consisting of Ga-Ga dimers is stabilized under N-rich conditions whereas metallic reconstructions are favorable under Ga-rich conditions. The H-terminated surface is stabilized over the wide range of growth conditions when the pressure of H_2 is high. We also reveal that several Mg-incorporated surfaces, in which one Mg atom substitutes for one of the topmost Ga atoms, can be formed under growth conditions. Under growth condition of metal-organic vapor-phase epitaxy, the H-terminated surface with Ga-Ga dimers and substitutional Mg is found to be stable for GaN(1$\bar{1}$01) surface, whereas the H-terminated surface without Mg can be formed for GaN(0001) surface. The orientation dependence in the stability of Mg incorporated surfaces provides a possible explanation for high Mg concentrations on semipolar GaN(1$\bar{1}$01) surface.

DOI: 10.1103/PhysRevB.81.245317 PACS number(s): 68.43.Bc, 68.43.Mn, 81.05.Ea

I. INTRODUCTION

The control of the charge-carrier concentration through doping is a key issue in many applications of group-III nitride semiconductors. The discovery of *p*-type conductivity in GaN using Mg doping leads to the widespread development of GaN-based optoelectronic device, such as light-emitting diodes, laser diodes, and photovoltaic cells.[1–4] However, GaN-based heterostructures are usually grown along the polar [0001] direction which has large polarization related electric field inside the multiquantum wells.[5] The internal electric fields in the spontaneous and piezoelectric polarization give rise to the quantum-confined Stark effect and reduce the radiative efficiency within the quantum wells. In order to reduce the effects of internal electric fields, there is an increasing interest in the crystal growth and device fabrication on semipolar orientations such as (11$\bar{2}$2), (10$\bar{1}$3), and (1$\bar{1}$01), due to their reduced and even negligible electric field.[6–15]

It has been recently found that the incorporation of Mg is more efficient on a GaN(1$\bar{1}$01) surface than on polar (0001) surfaces in addition to reduction of the internal electric fields: Mg concentrations on GaN(1$\bar{1}$01) surface measured by the secondary ion mass spectrometry (SIMS) are higher than that on polar (0001) surface.[13,15] However, the ideal GaN(1$\bar{1}$01) surface is N-terminated surface such as GaN(000$\bar{1}$) surface, in which the Mg doping efficiency is rather poor.[16] Therefore, the origins for high Mg concentrations on N-terminated GaN(1$\bar{1}$01) surface cannot be explained by the analogy with GaN(000$\bar{1}$) surface. To clarify the microscopic origin for high Mg concentrations on semipolar (1$\bar{1}$01) orientation, investigations for Mg-incorporation behavior as well as the reconstructions on the (1$\bar{1}$01) surfaces from theoretical viewpoints are necessary.

From theoretical viewpoints, the stability of Mg on GaN surfaces has been intensively investigated to address many of the issues raised by the experimental results. To explain the narrow window for smooth growth of GaN due to Mg on GaN(0001) surface,[17] the relative stabilities of possible Mg-rich reconstructions have been determined with respect to those of the clean surface, and the surface structures comprising 1/2–3/4 monolayer of Mg substituting for Ga in the top layer have been proposed in very Mg-rich conditions.[18] Sun *et al.*[19] have investigated the energetics of Mg adsorption and incorporation at GaN(0001) and (000$\bar{1}$) surfaces under a wide variety of conditions. They have clarified that the Mg incorporation is easier at the Ga-polar surface, but high Mg coverages tend to locally change the polarity from Ga to N polar. A thermodynamic approach with chemical potentials appropriate for realistic growth conditions has revealed that hydrogen stabilizes Mg-rich surface reconstructions for both GaN(0001) and (1$\bar{1}$00) surfaces.[20] To explain high hole concentrations in Mg-doped semipolar GaN(1$\bar{1}$0$\bar{1}$) surface,[10] the stability of Mg-incorporated GaN(1$\bar{1}$0$\bar{1}$) surface has also been examined.[21] In spite of these theoretical efforts, the Mg incorporation behavior and effects of hydrogen on the incorporation of Mg on semipolar GaN(10$\bar{1}$1) surface have never been studied at present.

In this study, we systematically investigate reconstruction and Mg-incorporation behavior on GaN(1$\bar{1}$01) surface by performing first-principles total-energy calculations. We predict surface phase diagrams as functions of temperature and Ga pressure, which is obtained by comparing the calculated adsorption energy with gas-phase chemical potential. We also reveal that one Mg atom can substitute the topmost Ga atom in the 2×2 reconstruction under growth conditions. The Mg-incorporated surfaces are stable both in the molecular-beam epitaxy (MBE) growth and metal-organic vapor-phase epitaxy (MOVPE) growth while the Mg can desorb for polar GaN(0001) surface in the case of MOPVE growth. The difference in the stability of Mg-incorporated surfaces depending on surface orientation provides a possible

explanation for experimentally observed high Mg concentrations on semipolar GaN($1\bar{1}01$) surface.

In the next section we describe our methodology, and Secs. III–V contain the main results and discussion. The surface reconstruction on GaN($1\bar{1}01$) surface under growth conditions is discussed in Sec. III. The stabilities of Mg-incorporated surfaces for low and high H_2 pressures are described in Secs. IV and V, respectively.

II. METHODOLOGY

Total-energy calculations are performed within plane-wave pseudopotential approach using the generalized gradient approximation.[22] We use norm-conserving pseudopotentials[23] for Ga and H atoms and ultrasoft pseudopotential[24] for N atoms. Ga $3d$ electrons are treated by partial core corrections.[25] The conjugate-gradient technique is utilized both for the electronic structure calculations and for geometry optimization.[26,27] The optimization of geometry is performed until the remaining forces acting on the atoms are less than 5.0×10^{-3} Ry/Å. The valence wave functions are expanded by the plane-wave basis set with a cut-off energy of 28 Ry.

GaN($1\bar{1}01$) surface is simulated using the 2×2 slab model consisting of eight atomic layers GaN and ~9 Å vacuum region. In order to compare the results of GaN($1\bar{1}01$) surface with those on polar GaN(0001) surface, we also adopt the 2×2 slab model consisting of four bilayer GaN along the [0001] direction and ~9 Å vacuum region. The bottom surface of the slab is passivated with artificial hydrogen atoms[28] and the lower four layers are fixed at ideal positions. We use eight k points sampling for the 1×1 surface unit, which provides sufficient accuracy in the total energy.[29] A variety of Mg-incorporated surface structures as well as those without Mg are considered to determine the stable surface structures under growth conditions.

The relative stability among various surface structures including Mg is determined using the formation energy E_f given by[18,19]

$$E_f = E_{tot} - E_{ref} - n_{\mathrm{Mg}}\mu_{\mathrm{Mg}} - n_{\mathrm{Ga}}\mu_{\mathrm{Ga}} - n_{\mathrm{N}}\mu_{\mathrm{N}} - n_{\mathrm{H}}\mu_{\mathrm{H}}, \quad (1)$$

where E_{tot} and E_{ref} are the total energy of the surface under consideration and of the reference surface, respectively, μ_i is the chemical potential of the ith species, and n_i is the number of excess or deficit ith atoms with respect to the reference. Here, we assume that the surface is in equilibrium with bulk GaN expressed as

$$\mu_{\mathrm{Ga}} + \mu_{\mathrm{N}} = \mu_{\mathrm{GaN}}^{\mathrm{bulk}}, \quad (2)$$

where $\mu_{\mathrm{GaN}}^{\mathrm{bulk}}$ is the chemical potential of bulk GaN. μ_{Ga} can vary in the thermodynamically allowed range $\mu_{\mathrm{Ga}}^{\mathrm{bulk}}+\Delta H_f \le \mu_{\mathrm{Ga}} \le \mu_{\mathrm{Ga}}^{\mathrm{bulk}}$, where ΔH_f is the heat of formation of bulk GaN ($\mu_{\mathrm{Ga}}^{\mathrm{bulk}}$ is the chemical potential of bulk Ga). The lower and the upper limits correspond to N-rich and Ga-rich conditions, respectively. The calculated value of ΔH_f is −1.24 eV, which agrees with previous calculations[18,19] and experiments.[30] The reconstructions under growth conditions, such as temperature and pressure, are determined using the surface phase diagrams, which are obtained by comparing the adsorption energy E_{ad} with the gas-phase chemical potential μ_{gas} given by[31,32]

$$\mu_{gas} = -k_B T \ln\left\{\frac{gk_BT}{p}\left(\frac{2\pi m k_B T}{h^2}\right)^{3/2} \times \zeta_{rot} \times \zeta_{vib}\right\}, \quad (3)$$

where k_B is the Boltzmann constant, T is the gas temperature, g is the degree of degeneracy of electron energy level, and p is pressure. ζ_{rot} and ζ_{vib} are the partition functions for rotational and vibrational motions, respectively. The structure corresponding to adsorbed surface is favorable when E_{ad} is less than μ_{gas}, whereas desorbed surface is stabilized when μ_{gas} is less than E_{ad}.

Since Mg-related precipitates such as magnesium nitride (Mg_3N_2) are formed under Mg-rich conditions, the thermodynamically allowed range for the chemical potential of Mg varies as $\mu_{\mathrm{Mg}} \le \mu_{\mathrm{Mg}}^{\mathrm{bulk}}$, where $\mu_{\mathrm{Mg}}^{\mathrm{bulk}}$ is the chemical potential of Mg in bulk Mg_3N_2. The value of $\mu_{\mathrm{Mg}}^{\mathrm{bulk}}$ can be calculated by assuming the surface in equilibrium with bulk Mg_3N_2 expressed as

$$3\mu_{\mathrm{Mg}}^{\mathrm{bulk}} + 2(\mu_{\mathrm{GaN}}^{\mathrm{bulk}} - \mu_{\mathrm{Ga}}) = \mu_{\mathrm{Mg_3N_2}}^{\mathrm{bulk}}. \quad (4)$$

Owing to this condition, the Mg-rich limit in μ_{Mg} is determined as a function of μ_{Ga}. The energy of bulk Mg_3N_2 is calculated using cubic unit cell containing 80 atoms. The calculated lattice constant (9.93 Å) agrees well with experimental value (9.96 Å) (Ref. 33) and recent calculated ones (9.86–9.99 Å).[18,19] The cohesive energy of Mg_3N_2 (−4.09 eV) compares well with that in previous calculation (−4.13 eV).[19]

III. RECONSTRUCTION ON CLEAN GaN($1\bar{1}01$) SURFACE

Figure 1 shows the surface formation energies for various structures on GaN($1\bar{1}01$) surfaces without Mg as a functions of μ_{Ga}. We have examined more than twenty different structures. This figure includes only those reconstructions that are found to be energetically favorable in some part of the phase space spanned by the chemical potentials. The ideal surface consisting of two- and three-coordinated N atoms shown in Fig. 2(a) is taken as the reference surface. When the pressure of H_2 is low (around $p_{\mathrm{H_2}}=1.0\times10^{-8}$ Torr at 1300 K, i.e., $\mu_{\mathrm{H}}=-2.3$ eV), this structure is stabilized under extreme N-rich conditions. The formation energies of H-terminated surfaces at $\mu_{\mathrm{H}}=-2.3$ eV are ~1.0 eV higher than that of the most stable surface (not shown here). Under moderate N-rich conditions, two-coordinated N atoms in the ideal surface are unstable. These N atoms desorb and four Ga-Ga dimers are formed at the topmost layer for $-1.17 \le \mu_{\mathrm{Ga}} \le -0.45$ eV [Fig. 2(b)]. Under extreme Ga-rich conditions, we find a number of metallic reconstructions depending on the chemical potential of Ga. The surface consisting of a Ga monolayer shown in Fig. 2(c) is favorable for $-0.45 \le \mu_{\mathrm{Ga}} \le -0.08$ eV, while the surface with a Ga bilayer is the most stable for $\mu_{\mathrm{Ga}} \ge -0.08$ eV. GaN($1\bar{1}01$) surface has similar

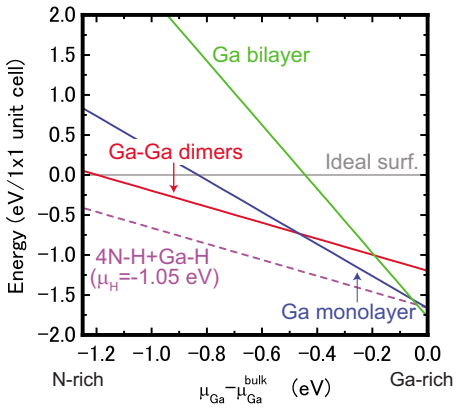

FIG. 1. (Color online) Calculated surface formation energies for various structures on GaN(1$\bar{1}$01) surface using Eq. (1) as a functions of μ_{Ga}. The formation energies of reconstructions that are found to be energetically favorable in some part of the phase space spanned by the chemical potentials are shown. The reconstructions with and without H atoms are represented by dashed and solid lines, respectively. The chemical potential of hydrogen (μ_H=−1.05 eV) for the formation energy of hydrogen-terminated surface (4N-H+Ga-H) corresponds to high H_2 pressure, p_{H_2}=76 Torr at 1300 K. The geometries are shown in Fig. 2.

tendency in the stabilization of metallic reconstruction under Ga-rich conditions to other surface orientation.[34–36] Therefore, in the case of MBE growth, a variety of reconstruction emerges depending on the growth conditions.

When we consider high H_2 pressure conditions which correspond to the case of MOVPE growth, the stable structures differ from those in low H_2 pressures. We obtain the hydrogen chemical potential μ_H=−1.05 eV using Eq. (3) for the pressure of H_2 around 76 Torr (0.1 atm) at 1300 K. In this condition, the surface in which all the topmost N atoms and one of topmost Ga atoms in the Ga-Ga dimers are terminated by H atoms [4N-H+Ga-H, the position of H atoms are

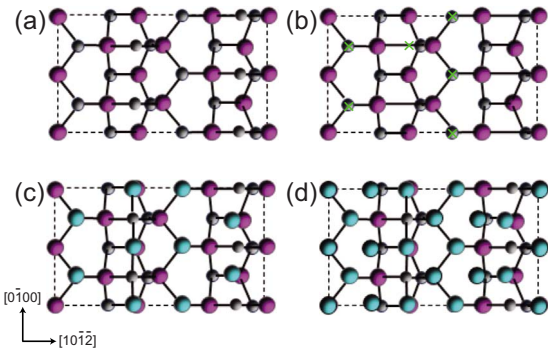

FIG. 2. (Color online) Schematic top views of (a) ideal cleavage GaN(1$\bar{1}$01) surface, and the surface consisting of (b) Ga-Ga dimers, (c) a Ga monolayer, and (d) a Ga bilayer. Large and small gray circles represent Ga and N atoms, respectively. The Ga atoms forming Ga monolayer and Ga bilayer are represented by blue circles. The positions of H atoms in the H-terminated surface (4N-H+Ga-H in Fig. 1) are marked by crosses in the surface consisting Ga-Ga dimers. The unit cell used in this study is shown by a dashed rectangle.

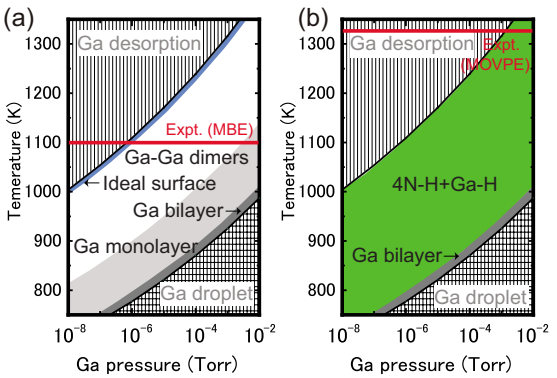

FIG. 3. (Color online) Surface phase diagram of GaN(1$\bar{1}$01) surface without Mg as functions of temperature and Ga pressure under (a) low ($p_{H_2}=1.0\times10^{-8}$ Torr) and (b) high (p_{H_2}=76 Torr) hydrogen pressures. The growth temperatures of GaN in the MBE and MOVPE (Refs. 13 and 15) are attached by red lines.

shown in Fig. 2(b)] is found to be stabilized over the wide chemical potential range of Ga. The surface with a Ga bilayer are stabilized only for $\mu_{Ga}\geq-0.04$ eV. This implies that the 4N-H+Ga-H usually appears during the MOVPE growth. It should be noted that the bonding states of Ga-Ga dimer and Ga-H bonds are completely occupied by the excess electrons caused by N-H bonds. Since there is no excess electron on the Ga dangling bonds, the stabilization of the 4N-H+Ga-H can be interpreted in terms of the electron counting (EC) rule,[37] as seen in the H-terminated GaN(0001) surface.[38]

The reconstructions of GaN(1$\bar{1}$01) surfaces under realistic conditions such as temperature and pressure can be discussed using the surface phase diagrams shown in Fig. 3. For low H_2 pressure conditions ($p_{H_2}=1.0\times10^{-8}$ Torr), as shown in Fig. 3(a), many types reconstructions can be realized depending temperature and Ga pressure. Around 1100 K (a typical MBE growth temperature), all the reconstructions obtained in the present calculations are expected to be found even though the temperature range for the stabilization of the ideal surface is very narrow. It is also suggested that the growth kinetics on the GaN(1$\bar{1}$01) surface depends on the growth temperatures owing to temperature-dependent surface reconstructions. When the pressure of H_2 is high (p_{H_2}=76 Torr), the H-terminated surface (4N-H+Ga-H) is stabilized and the surface with a Ga biliayer appears only for ~1000 K, as shown in Fig. 3(b). Considering that the growth temperatures of a typical MOVPE growth is around 1300 K, it is highly likely that GaN(1$\bar{1}$01) surface forms the H-terminated structure during the MOVPE growth.

IV. Mg INCORPORATION FOR LOW H_2 PRESSURES

Figure 4 depicts the diagram of stable structures on GaN(1$\bar{1}$01) surface including Mg as functions of μ_{Ga} and μ_{Mg} using Eq. (1) for low H_2 pressures, along with that on GaN(0001) surface for comparison. The boundary lines separating different regions correspond to chemical potentials for which two structures have the same formation energy. Here,

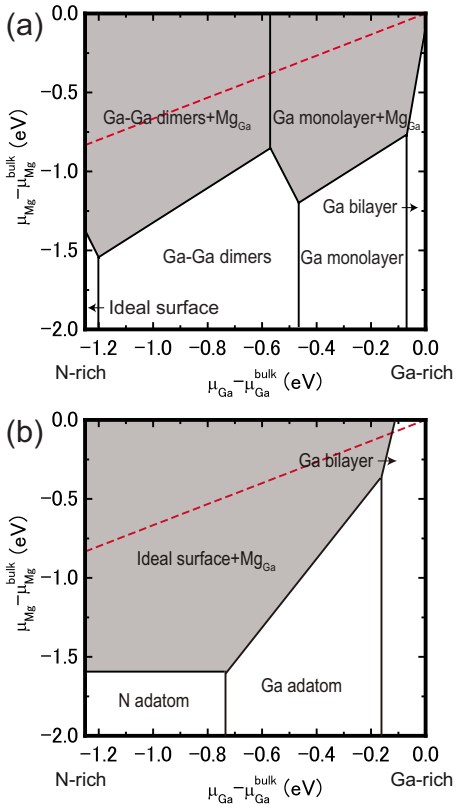

FIG. 4. (Color online) Stable structures on Mg-incorporated (a) GaN($1\bar{1}01$) and (b) GaN(0001) surfaces as functions of μ_{Ga} and μ_{Mg} for low H_2 pressures (μ_H=−2.3 eV). The stable regions of Mg-incorporated surfaces, such as Ga-Ga dimer+Mg_{Ga} and Ga monlayer+Mg_{Ga} are emphasized by shaded area. Geometries of Mg-incorporated GaN($1\bar{1}01$) surfaces are shown in Fig. 5. Dashed red lines denote the Mg-rich limit conditions expressed by Eq. (4).

we assume only one Mg atom in the unit cell because the partial pressure of Mg during doping should be much lower than that of Ga, i.e., the chemical potential of Mg is expected to vary much lower than the Mg-rich limit for Mg_3N_2 precipitation.[39] These diagrams clearly demonstrate that Mg atoms can be incorporated when μ_{Mg} is higher than −1.6 eV, depending on the chemical potential of Ga. For GaN($1\bar{1}01$) surface, as shown in Fig. 4(a), the surface with a substitutional Mg at one of Ga-Ga dimers [Ga-Ga dimers+Mg_{Ga} shown in Fig. 5(a)] can be stabilized for $\mu_{Ga} \leq -0.58$ eV while the surface with a Ga monolayer including Mg [Ga monlayer+Mg_{Ga} shown in Fig. 5(b)] is favorable under Ga-rich conditions ($\mu_{Ga} \geq -0.58$ eV). For GaN(0001) surface, the ideal surface with a substitutional Mg [ideal surface +Mg_{Ga} in Fig. 4(b)] is favorable over the wide chemical potential range of Ga if the chemical potential of Mg is lower than −0.5 eV.

Our inspection of the electronic structure also clarifies that the stabilization of the Mg-incorporated structure with Ga-Ga dimers on GaN($1\bar{1}01$) is basically interpreted in terms of the EC rule. In this case, five electrons are needed to satisfy the EC rule, and substituting one of Ga-Ga dimers by a Mg atom and the formation of one Ga dangling bond reduce the number of lacking electrons. This scenario is also

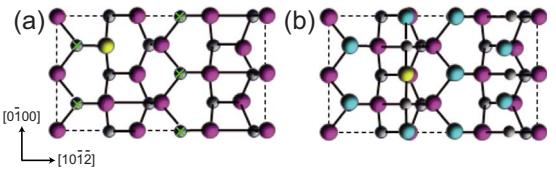

FIG. 5. (Color online) Schematic top views of Mg-incorporated GaN($1\bar{1}01$) surfaces with a substitutional Mg in (a) Ga-Ga dimers and (b) Ga monolayer, which are stabilized under N-rich and Ga-rich conditions, respectively. The notation of circles is the same as in Fig. 2. The Mg atoms are represented by yellow circles. The positions of H atoms in the H-terminated surface (4N-H+Mg_{Ga} in Fig. 4) are marked by crosses in the Mg-incorporated surface with Ga-Ga dimers.

applied on GaN(0001) surface. The substitutional Mg reduces the number of excess electrons on the ideal surface. However, the EC rule is no longer applicable for the surface with a Ga monolayer because this surface possesses metallic nature. The stabilization of this metallic surface with Mg might be due to the formation of stable metallic Ga-Mg bonds.

Furthermore, we estimate the stable temperature range of the Mg-incorporated surface under the N-rich limit. Here, the temperature for phase transition between Mg-incorporated and Mg-free surfaces is calculated by comparing the value of μ_{Mg} at the boundary line with the gas-phase chemical potential of Mg atom using Eq. (3). When the pressure of Mg is lower than 1.0×10^{-2} Torr, the transition temperatures are found to be 1010–1400 K for GaN($1\bar{1}01$) surface and 1050–1430 K for GaN(0001) surface: For low H_2 pressures, Mg atoms can be incorporated regardless of the growth orientation, indicating that high Mg concentrations can be obtained in both ($1\bar{1}01$) and (0001) orientations in the case of MBE growth. However, this differs from the SIMS measurements of GaN fabricated by the MOVPE growth, in which the concentrations of Mg on GaN($1\bar{1}01$) surface is higher than that on GaN(0001) surface.[13,15] Due to the presence of hydrogen, the incorporation behavior of Mg in the case of MOVPE growth is different from that in the MBE growth, as explained below.

V. Mg INCORPORATION FOR HIGH H_2 PRESSURES

We now consider the effects of hydrogen on the stability of Mg-incorporated surfaces. Figure 6 depicts the diagram of stable structures on GaN($1\bar{1}01$) surface including Mg atoms as functions of μ_{Ga} and μ_{Mg} using Eq. (1) for high H_2 pressures, along with that on GaN(0001) surface. These diagrams demonstrate that Mg atoms can be incorporated, but there is remarkable orientation dependence in the stable regions of the Mg-incorporated surfaces. As shown in Fig. 6(a), for GaN($1\bar{1}01$) surface the H-terminated surface with substitutional Mg (4N-H+Mg_{Ga}) are stabilized over the wide chemical potential range of Ga. Although the stable Mg-incorporated structure for high H_2 pressures is different from those for low H_2 pressures, trends in the stable region of

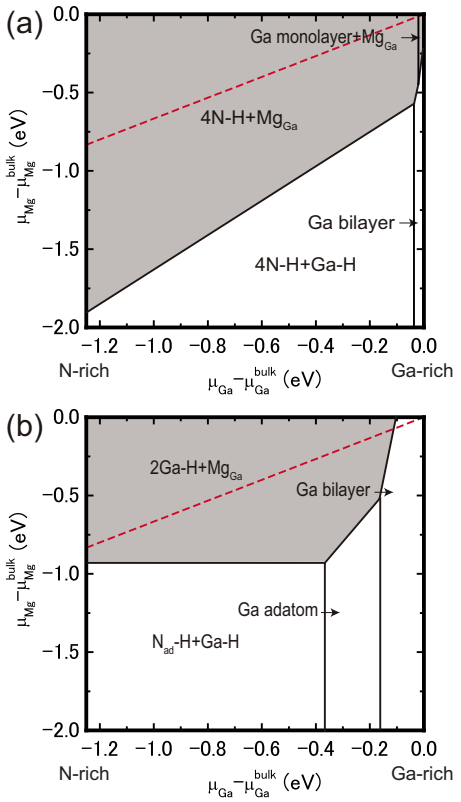

FIG. 6. (Color online) Stable structures on Mg-incorporated (a) GaN(1$\bar{1}$01) and (b) GaN(0001) surfaces as functions of μ_{Ga} and μ_{Mg} for high H_2 pressure (μ_H=−1.05 eV). The notation is the same as in Fig. 4.

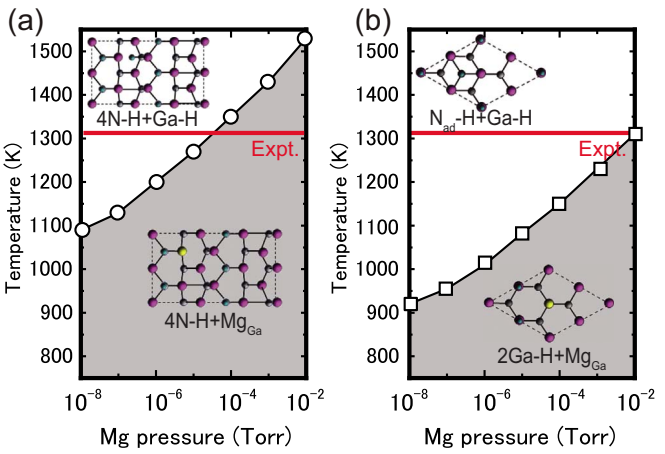

FIG. 7. (Color online) Temperatures for phase transition between Mg-incorporated and Mg-free surfaces in the N-rich limit (μ_{Ga}=−1.24 eV) as a function Mg pressure on (a) GaN(1$\bar{1}$01) and (b) GaN(0001) surfaces. The Mg-incorporated surfaces are stabilized in the regions emphasized by shaded area. Schematic views of surface structures are also shown. Large and small gray circles represent Ga and N atoms, respectively. The H and the Mg atoms are represented by small green and yellow circles, respectively. The growth temperature of GaN by the MOVPE in Refs. 13 and 15 is attached by red lines.

Mg-incorporated surfaces among the phase space spanned by the chemical potentials are similar with each other. In contrast, for GaN(0001) surface the stable region of Mg-incorporated surfaces is drastically reduced by the presence of hydrogen. For $\mu_{Mg} \leq -0.91$ eV, the H-terminated surface with N adatom [N_{ad}-H+Ga-H in Fig. 6(b)] is stabilized over the wide chemical potential range of Ga. This is because strong Ga-N and N-H bonds are formed in the N_{ad}-H+Ga-H, which simultaneously satisfies the EC rule. In the N-rich conditions, in particular, the stabilization of the N_{ad}-H+Ga-H narrows the μ_{Mg} range for which the Mg-incorporated surface is stabilized.

To discuss the orientation dependence in the stability of Mg-incorporated surfaces for high H_2 pressures more quantitatively, we here estimate temperatures for phase transition between Mg-incorporated and Mg-free surfaces in the N-rich limit. The calculation procedure is described in Sec. IV. Figure 7 shows the temperatures for phase transition on GaN(1$\bar{1}$01) and GaN(0001) surfaces at p_{H_2}=76 Torr. For GaN(1$\bar{1}$01) surface, the temperatures at p_{H_2}=76 Torr (1090–1530 K) are almost similar to those at $p_{H_2}=1.0\times10^{-8}$ Torr (1010–1400 K), as shown in Fig. 7(a). On the contrary, as shown in Fig. 7(b), the transition temperatures in GaN(0001) surface at p_{H_2}=76 Torr are ranging 930–1310 K, which are remarkably lower than those at $p_{H_2}=1.0\times10^{-8}$ Torr (1050–1430 K). The pressure dependence in the transition temperatures for GaN(0001) surface originates from the difference in the boundary line between the surfaces with and without Mg, leading to the orientation dependence in the transition temperature. The lower temperatures for the phase transition on GaN(0001) thus suggest that under the MOPVE growth around 1300 K the incorporation of Mg atoms on semipolar (1$\bar{1}$01) orientation is rather efficient than that on the polar (0001) orientation. Although the kinetics such as adsorption and desorption behavior of Mg during the growth processes should be verified, this efficient Mg incorporation results in high Mg concentrations on GaN(1$\bar{1}$01) surface, qualitatively consistent with the experimental results by the SIMS.[13,15]

VI. SUMMARY

We have investigated the surface reconstructions and Mg incorporation on GaN surfaces in semipolar (1$\bar{1}$01) orientation by performing first-principles pseudopotential calculations. Using the calculated total energies, we have predicted surface phase diagrams which manifest the appearance of several surface structures depending on the growth conditions. When the pressure of H_2 is low, the surface consisting of Ga-Ga dimers is stable under N-rich conditions whereas metallic reconstructions such as Ga monolayer and Ga bilayer are favorable under Ga-rich conditions. When hydrogen is present, the H-terminated surface is stabilized over the wide chemical potential range of Ga. Our calculations for Mg-incorporated surfaces have predicted several Mg-incorporated surfaces, in which one Mg atom substitutes one of the topmost Ga atoms. We have also found that hydrogen has a large effect on the stability, leading to the orientation

dependence in the stable conditions of Mg-incorporated surfaces. When the pressure of H_2 is low, Mg-incorporated surfaces such as Ga-Ga dimers+Mg_{Ga} and Ga monolayer +Mg_{Ga} are realized. The conditions for the stabilization of the H-terminated surface with substitutional Mg for high H_2 pressures are similar to those for low pressures on GaN($1\bar{1}01$) surface. In contrast, the stable conditions of Mg-incorporated surfaces under high H_2 pressures are rather severe for GaN(0001) surface due to the stabilization of the Mg-free surface with H-terminated N adatom, resulting in the orientation dependence. This provides a possible explanation of the experimental results in which GaN fabricated on semipolar ($1\bar{1}01$) orientation by the MOVPE growth exhibits rather high Mg concentrations.

ACKNOWLEDGMENTS

We would like to thank K. Hiramtsu and H. Miyake for their discussions and comments. This work was supported in part by a Grant-in-Aid for Scientific Research (Grant No. 21560032) from the Japan Society for the Promotion of Science. Computations were performed using Research Center for Computational Science (National Institutes of Natural Sciences).

*akiyama@phen.mie-u.ac.jp

[1] H. Amano, M. Kito, K. Hiramatsu, and I. Akasaki, Jpn. J. Appl. Phys., Part 2 **28**, L2112 (1989).
[2] S. Nakamura, T. Mukai, M. Senoh, and N. Iwasa, Jpn. J. Appl. Phys., Part 2 **31**, L139 (1992).
[3] C. Wang and R. F. Davis, Appl. Phys. Lett. **63**, 990 (1993).
[4] Z. Yang, L. K. Li, and W. I. Wang, Appl. Phys. Lett. **67**, 1686 (1995).
[5] F. Bernardini, V. Fiorentini, and D. Vanderbilt, Phys. Rev. B **56**, R10024 (1997).
[6] T. J. Baker, B. A. Haskell, F. Wu, P. T. Fini, J. S. Speck, and S. Nakamura, Jpn. J. Appl. Phys., Part 2 **44**, L920 (2005).
[7] M. Funato, M. Ueda, Y. Kawakami, Y. Narukawa, T. Kosugi, M. Takahashi, and T. Mukai, Jpn. J. Appl. Phys., Part 2 **45**, L659 (2006).
[8] M. Ueda, K. Kojima, M. Funato, Y. Kawakami, Y. Nakamura, and T. Mukai, Appl. Phys. Lett. **89**, 211907 (2006).
[9] J. F. Kaeding, H. Asamizu, H. Sato, M. Iza, T. E. Mates, S. P. DenBaars, J. S. Speck, and S. Nakamura, Appl. Phys. Lett. **89**, 202104 (2006).
[10] H. Zhong, A. Tyagi, N. N. Fellows, F. Wu, R. B. Chung, M. Saito, K. Fujito, J. S. Speck, S. P. DenBaars, and S. Nakamura, Appl. Phys. Lett. **90**, 233504 (2007).
[11] T. Hikosaka, N. Koide, Y. Honda, M. Yamaguchi, and N. Sawaki, Phys. Status Solidi C **3**, 1425 (2006).
[12] J. Saida, E. H. Kim, T. Hikosaka, Y. Honda, M. Yamaguchi, and N. Sawaki, Phys. Status Solidi C **5**, 1746 (2008).
[13] T. Hikosaka, N. Koide, Y. Honda, M. Yamaguchi, and N. Sawaki, J. Cryst. Growth **298**, 207 (2007).
[14] N. Sawaki, T. Hikosaka, N. Koide, S. Tanaka, Y. Honda, and M. Yamaguchi, J. Cryst. Growth **311**, 2867 (2009).
[15] K. Tomita, T. Hikosaka, T. Kachi, and N. Sawaki, J. Cryst. Growth **311**, 2883 (2009).
[16] L. K. Li, M. J. Jurkovic, and W. I. Wang, Appl. Phys. Lett. **76**, 1740 (2000).
[17] E. Monroy, T. Andreev, P. Holliger, E. Bellet-Amalric, T. Shibata, M. Tanaka, and B. Daudin, Appl. Phys. Lett. **84**, 2554 (2004).
[18] J. E. Northrup, Appl. Phys. Lett. **86**, 122108 (2005).
[19] Q. Sun, A. Selloni, T. H. Myers, and W. A. Doolittle, Phys. Rev. B **73**, 155337 (2006).
[20] J. E. Northrup, Phys. Rev. B **77**, 045313 (2008).
[21] T. Akiyama, D. Ammi, K. Nakamura, and T. Ito, Jpn. J. Appl. Phys. **48**, 110202 (2009).
[22] J. P. Perdew, K. Burke, and M. Ernzerhof, Phys. Rev. Lett. **77**, 3865 (1996).
[23] N. Troullier and J. L. Martins, Phys. Rev. B **43**, 1993 (1991).
[24] D. Vanderbilt, Phys. Rev. B **41**, 7892 (1990).
[25] S. G. Louie, S. Froyen, and M. L. Cohen, Phys. Rev. B **26**, 1738 (1982).
[26] J. Yamauchi, M. Tsukada, S. Watanabe, and O. Sugino, Phys. Rev. B **54**, 5586 (1996).
[27] H. Kageshima and K. Shiraishi, Phys. Rev. B **56**, 14985 (1997).
[28] K. Shiraishi, J. Phys. Soc. Jpn. **59**, 3455 (1990).
[29] The calculations with a cut-off energy of 36 Ry and 16 k points sampling have been performed to check the total-energy convergence. The adsorption and the desorption energies of Ga and N atoms in the ideal surface are found to be converged within 0.01 eV and 0.03 eV, respectively, which are much lower than the energy differences discussed in the present study.
[30] *CRC Handbook of Chemistry and Physics*, 80th ed., edited by D. R. Lide (CRC Press, Florida, 1999).
[31] Y. Kangawa, T. Ito, A. Taguchi, K. Shiraishi, and T. Ohachi, Surf. Sci. **493**, 178 (2001).
[32] Y. Kangawa, T. Ito, A. Taguchi, K. Shiraishi, T. Irisawa, and T. Ohachi, Appl. Surf. Sci. **190**, 517 (2002).
[33] D. E. Partin, D. J. Williams, and M. O'Keeffe, J. Solid State Chem. **132**, 56 (1997).
[34] D. Segev and C. G. Van de Walle, Surf. Sci. **601**, L15 (2007).
[35] T. Akiyama, D. Ammi, K. Nakamura, and T. Ito, Jpn. J. Appl. Phys. **48**, 100201 (2009).
[36] T. Yamashita, T. Akiyama, K. Nakamura, and T. Ito, Jpn. J. Appl. Phys. **48**, 120201 (2009).
[37] M. D. Pashley, K. W. Haberern, W. Friday, J. M. Woodall, and P. D. Kirchner, Phys. Rev. Lett. **60**, 2176 (1988).
[38] C. G. Van de Walle and J. Neugebauer, Phys. Rev. Lett. **88**, 066103 (2002).
[39] By taking account of different number of Mg atoms, we have obtained similar formation energies reported in the previous calculations for GaN(0001) surface. See Refs. 19 and 20.